Electronic properties of amorphous Zr_xT_{1-x} alloys (T=Cu, Ni, Pd, Pt, Co, or Rh)

H.-J. Eifert and B. Elschner
Institut für Festkörperphysik, Technische Hochschule Darmstadt, D-6100 Darmstadt, Federal Republic of Germany

K. H. J. Buschow
Philips Research Laboratories, 5600-JA, Eindhoven, The Netherlands
(Received 16 August 1983)

Amorphous Zr-rich alloys of the type Zr_xT_{1-x} with T=Cu, Ni, Pd, Pt, Co, and Rh were prepared by melt spinning. The thermal stability was studied by means of differential scanning calorimetry. The crystallization temperatures and the corresponding activation energies for crystallization were determined. The electronic properties of these alloys were investigated by means of susceptibility measurements and EPR measurements on Gd-doped samples. In combination with results on NMR measurements reported earlier, the present results made it possible to determine a value for the J_{fd} exchange constant (J_{fd}=0.1 eV) together with values of the density of states $N(E_F)$. In all alloys investigated $N(E_F)$ was found to be mainly due to the Zr d electrons, the various values lying within a few percent from the values $N(E_F)=0.88$ (eV atom spin)$^{-1}$.

I. INTRODUCTION

In a previous study we have used NMR together with magnetic measurements to investigate the electronic properties of amorphous alloys of the type Zr_xCu_{1-x}.[1] We have now supplemented these results with EPR measurements on similar alloys doped with small amounts of Gd. We also extended our investigation to other types of Zr_xT_{1-x} alloys where T represents Ni, Pd, Pt, Co, or Rh. What all these alloys have in common is that they show Pauli paramagnetism. They can be prepared straightforwardly by means of melt spinning, which has the advantage that the doping with Gd can be carried out to extremely low Gd concentrations and that the dope concentration is known to be within the same accuracy as in crystalline materials. This paper is organized as follows: The next section (Sec. II) deals with the preparation of the amorphous alloys, together with their characterization by means of x-ray diffraction and calorimetric measurements. Results of EPR measurements and magnetic measurements are described in Sec. III, and in Sec. IV these results are discussed together with results of the NMR investigation and results obtained for some of the alloys by means of specific-heat measurements.[2,3] In this section and also in Sec. V it will be evaluated how far the results obtained in the course of this investigation can enrich the results obtained elsewhere by means of photoemission studies and by means of band-structure calculations.

II. PREPARATION AND CHARACTERIZATION OF THE SAMPLES

The amorphous alloys investigated in this study were prepared in the form of small (2-mm) and thin ($\sim$30-μm) ribbons by means of melt spinning in an atmosphere of purified argon gas. For the melt spinning we used alloys of the desired composition which had previously been prepared by arc melting with starting materials of 99.99% purity for Ni, Co, Pt, Rh, Pd, Cu, and of 99.9% purity for Zr. All melt-spun alloys were examined by means of x-ray diffraction. Most alloys were found to give rise to x-ray diagrams composed of diffuse halos, characteristic of the amorphous state. Samples having sharp diffraction peaks superimposed on the diffuse halos were rejected from further physical examination.

The thermal stability of the alloys was investigated by means of differential scanning calorimetry (DSC), using again an atmosphere of purified argon. Upon heating the samples in the DSC unit a strong exothermic heat effect was observed, marking the transition from the amorphous to the crystalline state. The crystallization temperatures (T_x) corresponding to the temperatures of the exothermic DSC peaks measured with a heating rate s=50 K/min are listed for various alloys in Table I. The crystallization temperatures were found to vary appreciably with the heating rate, higher rates corresponding to higher T_x values. The dependence of T_x on s can be used to obtain

TABLE I. Crystallization temperatures (T_x) obtained by means of DSC with a heating rate of 50 K/min. The activation energies of ΔE were obtained from the slopes of the straight lines when $\ln(sT_x^{-1})$ is plotted versus T_x^{-1}; s is the heating rate.

Alloy	T_x (K)	ΔE (eV)
$Zr_{0.72}Cu_{0.28}$	666	2.70
$Zr_{0.67}Ni_{0.33}$	702	
$Zr_{0.67}Pd_{0.33}$	782	4.94
$Zr_{0.78}Pt_{0.22}$	810	
$Zr_{0.77}Pt_{0.23}$	824	4.66
$Zr_{0.67}Co_{0.33}$	722	4.87
$Zr_{0.80}Rh_{0.20}$	712	3.64
$Zr_{0.75}Rh_{0.25}$	741	4.21
$Zr_{0.74}Rh_{0.26}$	748	4.12
$Zr_{0.70}Rh_{0.30}$	758	4.73
$Zr_{0.66}Rh_{0.34}$	742	3.96

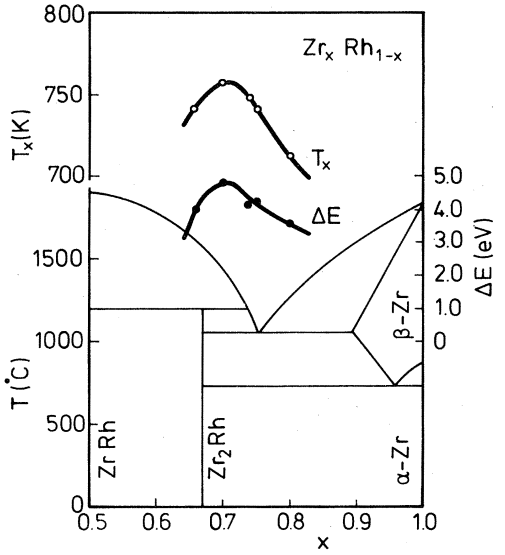

FIG. 1. Phase diagram of the Zr-Rh system and concentration dependence of the crystallization temperature (T_x) and activation energy for crystallization (ΔE).

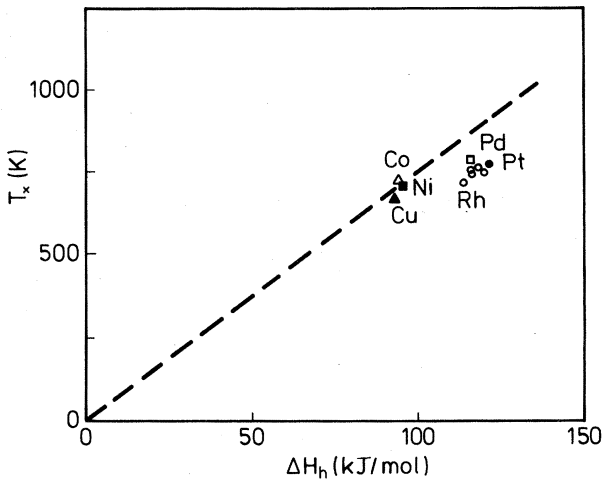

FIG. 2. Experimental crystallization temperatures of various Zr_xT_{1-x} alloys compared with model predictions. The dashed line represents the relation $T_x=7.5\Delta H_h$, where ΔH_h is the hole-formation energy.

values of the activation energy for crystallization (ΔE). Following the Kissinger and Boswell method we plotted $\ln(sT_x^{-1})$ vs T_x^{-1}.[4,5] Straight lines were obtained from the slope of which values of ΔE were derived.

These values are included in Table I. The concentration dependence of T_x and ΔE for the Zr_xRh_{1-x} alloys is displayed in the top part of Fig. 1. This concentration dependence can be compared with features of the Zr-Rh phase diagram[6] shown in the lower part of Fig. 1. It can be seen that the range of easy-glass formation is located close to the deep eutectic, as is commonly observed.[7,8] It is interesting to note that the alloy showing the highest crystallization temperature and the highest thermal stability does not correspond to the eutectic composition but to a slightly higher Rh concentration. It should also be noted that the activation energies for crystallization are considerably higher than the activation energy (0.86 eV) found for the relaxation of the amorphous state in $Zr_{0.75}Rh_{0.25}$ by Drehman and Johnson.[9] The latter relaxation involves only subtle atomic rearrangements, whereas in the amorphous-to-crystalline transformation long-range diffusion of atoms is required.

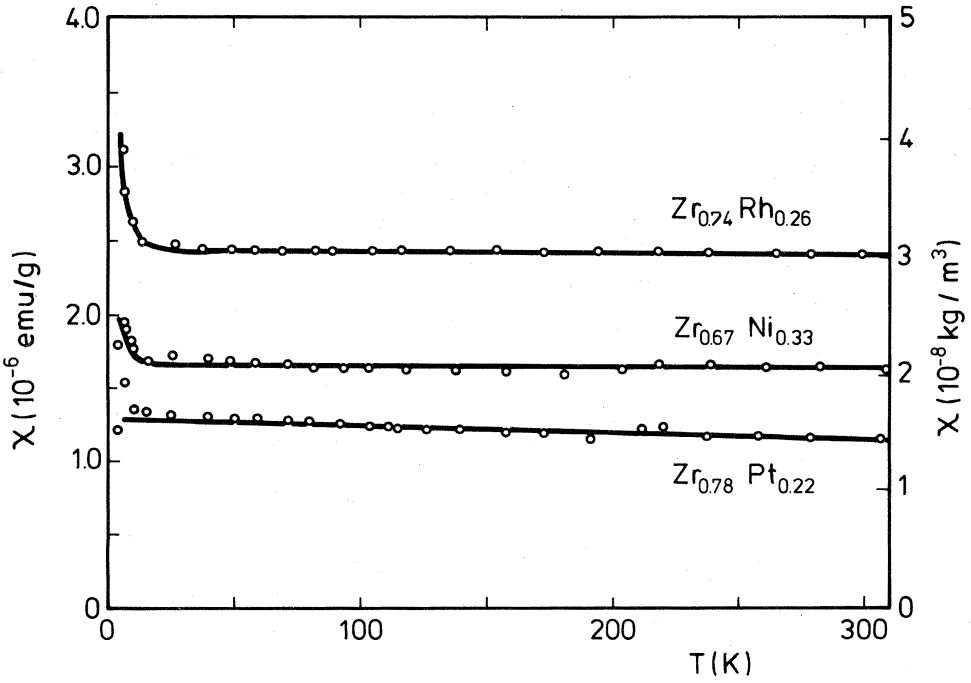

FIG. 3. Temperature dependence of the magnetic susceptibility in various Zr-based amorphous alloys.

TABLE II. Magnetic susceptibility corrected for diamagnetism ($\chi_{expt}-\chi_{dia}$) for various amorphous alloys. The quantity $(\chi_d+\chi_{vv})_T$ represents the surplus susceptibility in Eq. (1) when Cu in Zr_xCu_{1-x} is replaced by a T metal having an open d band.

Alloy	$\chi_{expt}-\chi_{dia}$ (10^{-4} emu/mol)	$(\chi_d+\chi_{vv})_T$(10^{-4} emu/mol)
$Zr_{0.72}Cu_{0.28}$	1.31±0.07	
$Zr_{0.67}Ni_{0.33}$	1.45±0.06	0.68
$Zr_{0.67}Pd_{0.33}$	1.43±0.05	0.62
$Zr_{0.78}Pt_{0.22}$	1.59±0.08	0.78
$Zr_{0.67}Co_{0.33}$	2.28±0.06	3.20
$Zr_{0.74}Rh_{0.26}$	2.43±0.07	4.16

The values of T_x listed in Table I are within 30 K of those reported by Rapp *et al.*[10] for Zr_xT_{1-x} alloys (T=Co, Ni, Cu) of similar concentration. Taking into consideration that the heating rate used by Rapp *et al.* is slightly lower (40 K/min) and that their Zr concentrations are slightly higher, the agreement between the two sets of data is quite satisfactory. Our value $T_x=782$ K for $Zr_{0.67}Pd_{0.33}$ deviates somewhat more from their result $T_x=720$ K for $Zr_{0.70}Pd_{0.30}$ to be explainable in terms of the small differences in heating rate and composition.

It has been shown elsewhere that the crystallization temperatures can be predicted on the basis of a model where the T_x values are expressed by means of the relation $T_x=c\,\Delta H_h$, where c is a constant between 7 and 8 when T_x is expressed in K and ΔH_h is expressed in kJ/mol.[11] The quantity ΔH_h represents the formation enthalpy of a hole, the size of the smaller type of atom in the binary amorphous alloys. It can be calculated straightforwardly[11] by using values of the monovacancy energies of the pure metals listed by Miedema.[12] In Fig. 2 experimental results and model predictions are compared, the dashed line representing the relation $T_x=7.5\Delta H_h$. It can be seen from the figure that the alloys studied in the course of the present investigation essentially behave according to the expectations based on the model.

III. MAGNETIC SUSCEPTIBILITY AND EPR

The magnetic susceptibility (χ) of the amorphous Zr_xT_{1-x} alloys was measured in the range 4.2–300 K on a vibrating sample magnetometer. Typical examples of results of such measurements are shown in Fig. 3. The alloys can be characterized as showing temperature-independent Pauli paramagnetism: The χ values after correction for diamagnetic contributions (χ_{dia}) have been listed in the second column of Table II. The diamagnetic contribution χ_{dia} was obtained by using a weighted average of the diamagnetic contributions of the pure elements.[13,14] The corrected susceptibility $\chi_{expt}-\chi_{dia}$ can then be decomposed into the following contributions:

$$\chi_{expt}-\chi_{dia}=\tfrac{2}{3}\chi_{s,p}+x(\chi_d+\chi_{vv})_{Zr}+(1-x)(\chi_d+\chi_{vv})_T\ . \quad (1)$$

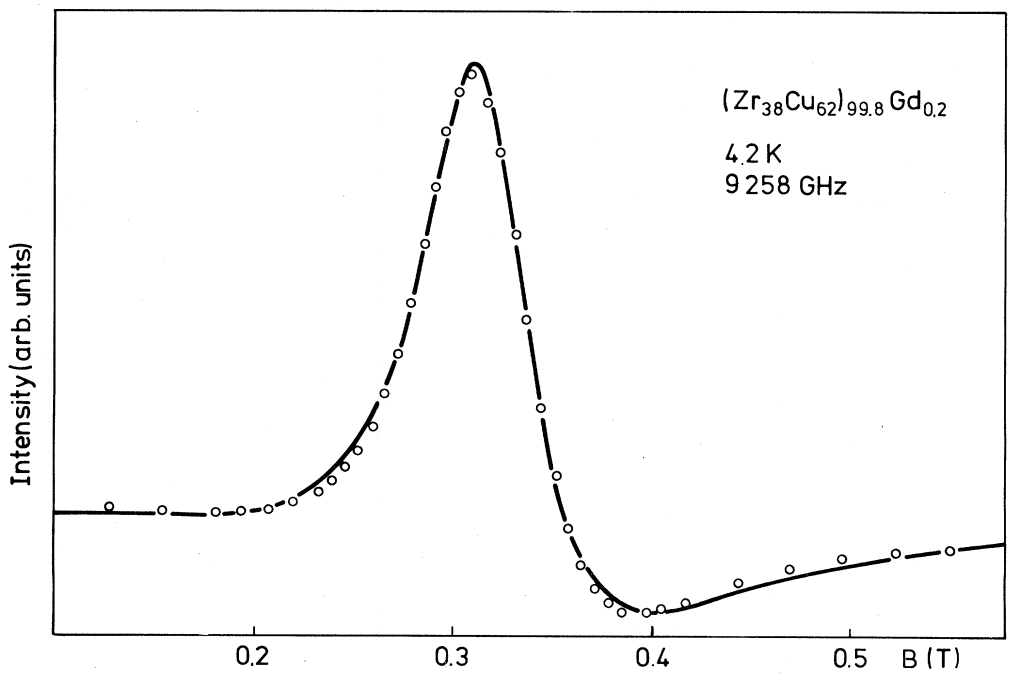

FIG. 4. EPR spectrum of amorphous $Zr_{0.38}Cu_{0.62}$ doped with 0.2% Gd. The solid line represents a fit of Lorentzian shape.

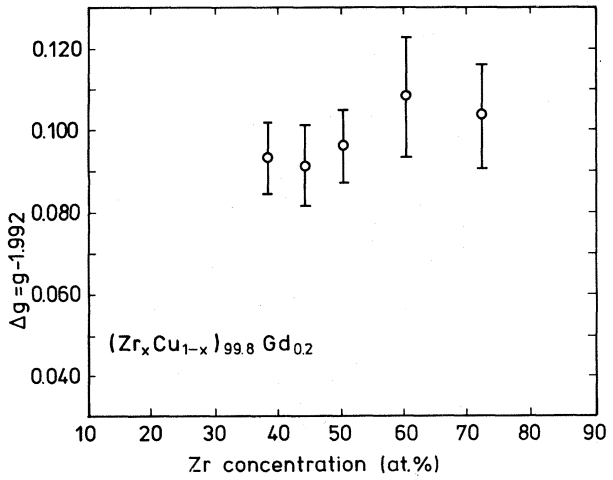

FIG. 5. Concentration dependence of the g shift in various amorphous Zr_xCu_{1-x} alloys doped with 0.2% Gd.

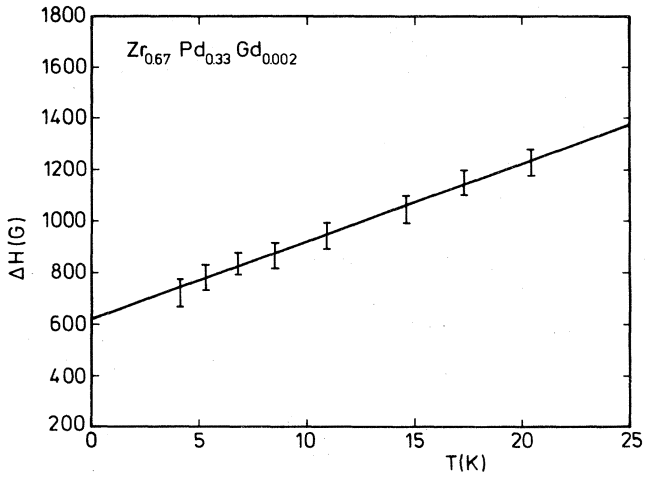

FIG. 6. Temperature dependence of the EPR line in Gd-doped amorphous $Zr_{0.67}Pd_{0.33}$.

In this expression the subscript Zr refers to the contribution of the Zr atoms while the subscript T refers to the additional contribution associated with the presence of the T atoms. The quantities $\chi_{s,p}$, χ_d, and χ_{vv} refer to the contributions of s,p electrons, d electrons, and the Van Vleck term, respectively. (Such a decomposition of the susceptibility into separate d-electron contributions due to Zr and T atoms is indicated by photoemission results and band-structure calculations; see below.) In a previous paper we investigated Zr_xCu_{1-x} alloys.[1] By combining results of $^{63}Cu(^{65}Cu)$ and ^{91}Zr NMR with results of susceptibility measurements we were able to determine the contributions $\chi_{s,p}$, $(\chi_d)_{Zr}$, and $(\chi_{vv})_{Zr}$ separately.

It was derived from our analysis that $\chi_{s,p}$ is nearly an order of magnitude smaller than χ_d and χ_{vv}. The term χ_{vv} was found to vary only slightly with concentration, in contrast to χ_d which increased strongly with x. Since the contribution $(\chi_d+\chi_{vv})_T$ is absent in Zr_xCu_{1-x} alloys one may use these results to obtain a rough estimate of the third term on the right-hand side of Eq. (1) by inserting the appropriate values of x and $(\chi_d+\chi_{vv})_{Zr}$ found in Zr_x-Cu_{1-x}. The values $(\chi_d+\chi_{vv})_T$ obtained in this way have been listed in the third column of Table II. These values suggest that the contribution of the T atoms in the alloys with T=Ni, Pd, and Pt is rather modest, whereas it is rather strong in the alloy based on Co and Rh.

The EPR measurements were made on a Varian spectrometer (E-line, X-band) in the temperature range 4.2–40 K using Zr_xT_{1-x} alloys doped with 0.2% of Gd. For the various alloy systems Zr_xT_{1-x} (T=Ni, Pd, Pt, Co, or Rh) in each case only a single alloy was studied, close in composition to $x=0.7$. In order to be able to make contact with the results obtained previously by means of NMR and χ measurements in the system Zr_xCu_{1-x} we extended our EPR investigation to four different concentrations for the Cu-base alloys. A typical EPR spectrum is shown in Fig. 4. The g values derived from these spectra have been used in Fig. 5 where the g shift $\Delta g=g_{expt}-1.992$ is plotted as a function of Zr concentration. The g values and g shifts of amorphous Zr_xT_{1-x} alloys of various different T components are compared in Table III. Note that the Δg values are rather high. They are about an order of magnitude higher than those found for Gd impurities in amorphous Pd-Si alloys.[15] Equally high Δg values were observed, for instance, for Gd impurities in metals such as La and Sc.[16] We also measured the temperature dependence of the linewidth ΔH. A typical example of such measurements is shown in Fig. 6. The linewidth is seen to increase linearly with temperature. From the slope of these lines we derived the Korringa rate $d\Delta H/dT$ and from its intercept with the vertical axis we obtained the residual linewidth ΔH_0. Both quantities have been listed for the various Zr_xT_{1-x} alloys in Table III. For the Zr_xCu_{1-x} alloys we have plotted the Korringa rate as a function of concentration in Fig. 7.

TABLE III. Korringa rates $d(\Delta H)/dT$, residual linewidths (ΔH_0), g values, g shifts (Δg), and Korringa ratios (R) in various Gd-doped amorphous alloys.

Alloy	$\frac{d\Delta H}{dT}$(G K^{-1})	ΔH_0 (G)	g	Δg	R
$Zr_{0.72}Cu_{0.28}$	36.2±2.5	610±20	2.095±0.014	0.103±0.014	0.15
$Zr_{0.67}Ni_{0.33}$	39.1±1.0	610±11	2.106±0.017	0.114±0.017	0.14
$Zr_{0.67}Pd_{0.33}$	30.1±2.0	614±20	2.104±0.010	0.112±0.010	0.11
$Zr_{0.78}Pt_{0.22}$	37.2±4.0	1060±70	2.111±0.040	0.119±0.040	0.12
$Zr_{0.67}Co_{0.33}$	30.0±5.0	920±80	2.113±0.026	0.121±0.026	0.09
$Zr_{0.74}Rh_{0.26}$	35.4±4.1	690±50	2.128±0.020	0.136±0.020	0.09

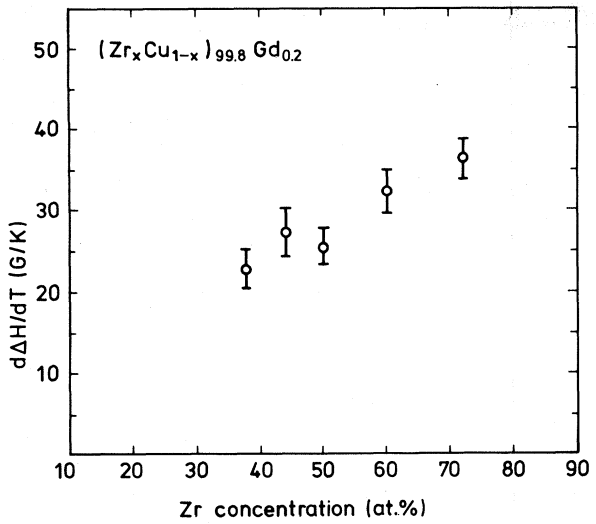

FIG. 7. Concentration dependence of the Korringa rate $d(\Delta H)/dT$ in various amorphous Zr_xCu_{1-x} alloys doped with 0.2% Gd.

IV. DISCUSSION

The results described in the preceding section can be used to obtain information on the density of states in these amorphous alloys. In terms of a two-band model the quantities Δg and $d(\Delta H)/dT$ can be given by[17]

$$\Delta g = J_{fs}N_s(E_F) + J_{fd}N_d(E_F) , \tag{2}$$

$$\frac{d(\Delta H)}{dT} = \frac{\pi k \mu_B}{g}[J_{fs}^2 N_s^2(E_F) + F_d J_{fd}^2 N_d^2(E_F)] . \tag{3}$$

The quantities J_{fs} and J_{fd} represent the exchange constants of the Gd $4f$ electrons with conduction electrons of s and d character, respectively. Both of these constants are usually of the order of magnitude of 0.1 eV. Here we note that the constants J appearing in Eq. (2) need not be the same as those in Eq. (3) owing to a difference in wave-number dependence.[18]

The quantities $N_s(E_F)$ and $N_d(E_F)$ are the corresponding densities of states at the Gd sites. The factor F_d accounts for the degeneracy of the d-band states. A value $F_d = 0.2$ is usually considered as appropriate.[19,20] Equations (2) and (3) only hold in cases where bottleneck effects are absent. This was not checked separately in the present alloys systems, but in view of the rather low Gd concentrations applied (0.2%) and the relatively high Δg values we assume that such effects are of less importance. Malozemoff *et al.*[21] studied EPR in amorphous $(Gd,Y)_{0.33}Al_{0.67}$ and found that Gd concentrations of less than 0.1% were required to open the bottleneck. However, in Zr_xT_{1-x} the situation is less favorable for the occurrence of a bottleneck in view of the higher spin-orbit splitting constant of Zr if compared to Y, the higher concentration of the $4d$ metal and the somewhat lower position of the Zr d band as compared to the Y d bands. The latter two features are probably also the reason that in amorphous Zr_xCu_{1-x}, unlike amorphous $Y_{0.33}Al_{0.67}$, the contributions of s electrons to $N(E_F)$ are roughly an order of magnitude smaller than the contributions of d electrons. For Zr_xCu_{1-x} this result was obtained by means of NMR measurements and has been reported elsewhere.[1] In the case of a prevailing d-electron density of states, using $F_d = 0.2$, one expects the Korringa ratio

$$R = \frac{d(\Delta H)/dT}{(\Delta g)^2 \pi k/(g\mu_B)} \tag{4}$$

to be of the order of 0.1. Comparison with the experimental R values listed in the last column of Table III shows that such a situation is found in the present amorphous alloys. Since the first term in Eq. (3) is more than an order of magnitude lower than the second term we may neglect it and write

$$N_d^2(E_F) \approx \frac{g}{0.2\pi k \mu_B} \frac{d(\Delta H)}{dT} J_{fd}^{-2} . \tag{5}$$

The values for $N_d(E_F)$ calculated in this way, using the experimental $d(\Delta H)/dT$ values and $J_{fd} = 0.1$ eV, are listed in the third column of Table IV.

For the Zr_xCu_{1-x} alloys we are in the fortunate position that the d-electron susceptibility χ_d was determined previously by combining magnetic and NMR data. We may then use the expression

$$N_d(E_F) = \chi_d / 2\mu_B^2 N \tag{6}$$

to obtain an independent check on the $N_d(E_F)$ values estimated by means of Eq. (5). The experimental χ_d values obtained previously and the corresponding $N_d(E_F)$ values are given in Table IV (fourth and fifth columns). As a second check we have included in the last column of Table IV the densities of states obtained by means of the expression

TABLE IV. Experimental values of the Korringa rates (in G K^{-1}) and d-electron susceptibilities (in emu/mole) in various amorphous Zr_xCu_{1-x} alloys. The corresponding values for the densities of states (in eV^{-1} per atom per spin) are indicated by $N_d^{\Delta H}(E_F)$ and $N_d^{\chi}(E_F)$, respectively. The value $N^{\gamma}(E_F)$ was derived from specific-heat data (see text).

Zr_xCu_{1-x}	$\frac{d\Delta H}{dT}$	$N_d^{\Delta H}(E_F)$	χ_d	$N_d^{\chi}(E_F)$	$N^{\gamma}(E_F)$
x					
0.72	36.2	0.90	5.93×10^{-5}	0.92	0.93
0.50	25.5	0.73	4.37×10^{-5}	0.68	0.70
0.44	27.0	0.76	4.08×10^{-5}	0.63	
0.38	22.8	0.70	3.69×10^{-5}	0.57	

$$N(E_F)=3\gamma/\pi^2k^2\,, \tag{7}$$

where we have used the values of the electronic coefficient of the specific heat γ determined for $Zr_{0.74}Cu_{0.26}$ and $Zr_{0.50}Cu_{0.50}$ by Samwer.[2]

It can be seen from the results shown in Table IV that there is good agreement between the three sets of independent values of the density of states for the alloys $x=0.72$ and 0.50. For the Cu-rich alloys only two sets of values for the density of states are listed. Here, too, the agreement is still satisfactory, the deviations being of the order of 20%.

The above results can also be interpreted as meaning that for the Zr-rich alloys the J_{fd} exchange constant is to a rather good approximation equal to 0.10 eV, whereas for the Cu-rich alloys its value tends to be slightly higher (0.12 eV). Inspection of the values of the Korringa rates listed in Table III shows that these remain more or less constant in the various amorphous Zr_xT_{1-x} alloys. In connection with Eq. (5) this means that variations in the values for J_{fd} and N_d roughly compensate or that these latter two quantities do not vary much in this series of alloys. Assuming that J_{sf} has the same value (0.1 eV) as found in $Zr_{0.72}Cu_{0.28}$ one may use Eq. (5) for calculating $N_d(E_F)$, using the experimental values of the Korringa rates.

The $N_d(E_F)$ values obtained in this way are listed in Table V, together with the corresponding Korringa rates. As far as they are available we have included values in the Table derived for the density of states by means of specific-heat measurements. It is interesting to note that all these values are considerably higher than the density of states 0.64 eV^{-1} per atom per spin derived from specific-heat measurements for pure Zr metal.[22]

Finally we wish to discuss the surplus susceptibility $(\chi_d+\chi_{vv})_T$ listed in Table II for the amorphous Zr_xT_{1-x} alloys in which T represents a late transition metal with an open d band. A comparison of the χ data in Table II with the $d(\Delta H)/dT$ data in Table III shows that the increase over the value found in the Cu alloy is not correlated with a similar increase in $d(\Delta H)/dT$. In other words, the surplus susceptibility does not contribute to the Korringa rate. This can be taken as evidence that the main part of the surplus susceptibility is due to an increase in the χ_{vv} contribution. In metallic systems an analog of the Van Vleck susceptibility was discussed by Kubo and Obata.[23] Typical values for this so-called orbital paramagnetism in nonmagnetic intermetallic compounds of d transition metals are of the order of 5.10^{-4} emu/mol.[24]

V. CONCLUDING REMARKS

By combining results of susceptibility measurements and EPR measurements with earlier results obtained by means of NMR we have been able to derive fairly accurate values for the density of states in amorphous Zr_xCu_{1-x} alloys and also for several alloys of the type Zr_xT_{1-x}, where T is a (late) transition metal. We showed that the density of states is primarily due to the d electrons of the Zr subband. It is fairly insensitive to the nature of the T component and about 30% larger than in pure crystalline Zr metal.

TABLE V. Experimental values of the Korringa rate (in GK^{-1}) in various amorphous alloys and the corresponding value of the density of states (in eV^{-1} per atom per spin). The two values in the last column were derived from specific-heat data published by Samwer (Ref. 2) and Graebner *et al.* (Ref. 3).

Alloy	$\frac{d\Delta H}{dT}$	$N_d(E_F)$	$N(E_F)$
$Zr_{0.72}Cu_{0.28}$	36.2	0.90	0.93
$Zr_{0.67}Ni_{0.33}$	39.1	0.94	
$Zr_{0.67}Pd_{0.33}$	30.1	0.82	1.07
$Zr_{0.78}Pt_{0.22}$	37.2	0.92	
$Zr_{0.67}Co_{0.33}$	30.0	0.82	
$Zr_{0.74}Rh_{0.26}$	35.4	0.90	

It is interesting to compare these findings with results obtained by means of photoelectron spectroscopy.[25] The main features of these latter results on Zr_xT_{1-x} alloys can be summarized as follows: The d bands of Zr and the late transition metal T do not coalesce into a common d band, which excludes a description of the magnetic and electronic properties of these materials in terms of a rigid-band approach. The photoemission spectra are dominated by two separate peaks associated with the d bands of the two components Zr and T. Both d bands have become narrower than found with the parent metals. Apart from this effect, the hybridization between the two sets of d states has also led to a repulsion between the two d bands, the Zr d band moving to higher energies (lower binding energies) and the d band due to the T electrons moving to lower energies (higher binding energies).[25,26] The concomitant hybridization leads to some d-electron sharing between the Zr and T atoms and increases somewhat the contribution of the d states due to T in the Zr d-band region. Owing to the shift in downward direction with respect to E_F the d bands of T components having a partially depleted d band will become more filled. As a consequence of this latter feature the partial density of states of the T component will be reduced considerably. Band-structure calculations showed that the density of states near the Fermi level is mainly determined by the Zr d band.[26] These results are in agreement with the results found in the present investigation.

Band-structure calculations have also shown that the partial d density of states due to Zr has a minimum slightly above E_F and increases below E_F.[26] Owing to the d-band repulsion mentioned above, one would expect therefore that as a consequence of the Zr d-band shift towards higher energies the Fermi level would move into a region of a higher d density of states. This is exactly what our results suggest, since we found an increase in $N_d(E_F)$ in the amorphous alloys relative to pure Zr metal. In this respect our results are somewhat different from the photoemission results[25] where the normalization of the photoemission spectra of Zr and the Zr_xT_{1-x} alloys does not suggest a substantial increase in the density of states.

[1]H.-J. Eifert, B. Elschner, and K. H. J. Buschow, Phys. Rev. B 25, 7441 (1982).
[2]K. Samwer, Ph.D thesis, University of Göttingen, 1981 (unpublished).
[3]J. E. Graebner, B. Golding, R. J. Schutz, F. S. L. Hsu, and H. S. Chen, Phys. Rev. Lett. 39, 1480 (1977).
[4]H. E. Kissinger, Anal. Chem. 29, 1702 (1957).
[5]F. G. Boswell, J. Therm. Anal. 18, 353 (1980).
[6]W. G. Moffat, *The Handbook of Binary Phase Diagrams* (General Electric, Schenectady, New York, 1978).
[7]H. S. Chen, Rep. Prog. Phys. 43, 353 (1980).
[8]R. W. Cahn, Contemp. Phys. 21, 43 (1980).
[9]A. J. Drehman and W. L. Johnson, Phys. Status Solidi A 52, 499 (1979).
[10]O. Rapp, B. Lindberg, H. S. Chen, and K. V. Rao, J. Less-Common Met. 62, 221 (1978).
[11]K. H. J. Buschow, Solid State Commun. 43, 171 (1982).
[12]A. R. Miedema, Z. Metallkd. 70, 345 (1979).
[13]Landolt-Börnstein, *Zahlenenueerte und Funktionen, New Series II/8,* edited by K. H. Hellwege (Springer, Berlin, 1964), Suppl. 1, p. 27.
[14]P. W. Selwood, *Magnetochemistry* (Interscience, New York, 1956), p. 73.
[15]K. H. J. Buschow, H.-J. Eifert, and B. Elschner, Phys. Status Solidi B 115, 455 (1983).
[16]R. H. Taylor, Adv. Phys. 24, 681 (1975).
[17]Y. Yafet and V. Jaccarino, Phys. Rev. 133, A1630 (1964).
[18]D. Davidov, K. Maki, R. Orbach, C. Rettori, and E. P. Chock, Solid State Commun. 12, 621 (1973).
[19]B. Caroli, P. Lederer, and D. Saint-James, Phys. Rev. Lett. 23, 700 (1969).
[20]L. Dworin and A. Narath, Phys. Rev. Lett. 25, 1287 (1970).
[21]A. P. Malozemoff, G. Suran, and R. C. Taylor, Phys. Rev. B 24, 2731 (1981).
[22]G. D. Kneip, Jr., J. O. Betterton, Jr., and J. O. Scarbrough, Phys. Rev. 130, 1687 (1963).
[23]R. Kubo and Y. Obata, J. Phys. Soc. Jpn. 11, 547 (1956).
[24]A. M. Clogston, A. C. Gossard, V. Jaccarino, and Y. Yafet, Phys. Rev. Lett. 9, 262 (1962).
[25]P. Oelhafen, E. Hauser, H.-J. Güntherodt, and K. H. Bennemann, Phys. Rev. Lett. 43, 1134 (1979).
[26]J. Kübler, K. H. Bennemann, R. Lapka, F. Rösel, P. Oelhafen, and H.-J. Güntherodt, Phys. Rev. B 23, 5176 (1981).